

# QCD sum rule analysis for light vector and axial-vector mesons in vacuum and nuclear matter

Stefan Leupold

*Institut für Theoretische Physik, Universität Giessen, D-35392 Giessen, Germany*

(Received 8 January 2001; published 14 June 2001)

Extending previous work we study the constraints of QCD sum rules on mass and width of light vector and axial-vector mesons in vacuum and in a medium with finite nuclear density. For the latter case especially the effect of nuclear pions leading to vector–axial-vector mixing is included in the analysis. We examine the consequences of the mixing effect for positions and shapes of the peaks which show up in the current-current correlators. We also discuss the model dependences in the amount of mixing, in the evaluation of the four-quark condensate, and in the width parametrizations for the meson spectral functions.

DOI: 10.1103/PhysRevC.64.015202

PACS number(s): 14.40.Cs, 21.65.+f, 11.30.Rd, 24.85.+p

## I. INTRODUCTION

One of the main goals of modern nuclear physics is to study the behavior of nuclear matter under extreme conditions. At low temperatures and densities the quarks and gluons as the basic constituents of strongly interacting matter form hadrons due to the confinement mechanism. In addition, the appearance of rather light mesons (pions and kaons) signals the existence of a spontaneously broken symmetry, the chiral symmetry. In fact this symmetry is approximately realized in the QCD Lagrangian. Another important hint that chiral symmetry is spontaneously broken in the vacuum state is the absence of chiral partners with equal masses. In a chirally symmetric state chiral partners would have the same mass. This concerns for example the isovector-vector meson  $\rho$  and its much heavier partner, the isovector–axial-vector meson  $a_1$ . It is expected that at high enough temperatures and densities confinement is lifted and chiral symmetry restored. High-energy heavy-ion collisions are dedicated to the creation of this new state of matter, the quark-gluon plasma (QGP) [1]. Unfortunately, even if such an ultrahot system of quarks and gluons is created only its decay products—which of course are hadrons and not deconfined quarks and gluons—can reach the detectors. Thus, the proof for the existence of this new stage of matter has to be performed rather indirectly. In addition to the observable hadrons also photons and dileptons are radiated from the hot fireball. These particles deserve special attention since they do not suffer from strong final state interactions. Therefore, once created in the high density region they are capable to carry information from that region to the detectors. Altogether, the challenge is to find unambiguous signs that (part of) the observed spectra of hadrons, photons, and dileptons are caused by the transient existence of the QGP. Clearly, to prove the existence of the QGP it is necessary to show that the spectra cannot be explained by a hot fireball made out of conventional interacting hadrons. This task is especially complicated by the fact that there is no straightforward derivation of hadronic Lagrangians from QCD as the underlying theory of strong interactions. Therefore it is not *a priori* clear how far one can trust in-medium calculations with hadronic Lagrangians as their parameters are adjusted to the description of vacuum processes. Connections between hadronic models and concepts on the one hand and QCD or QCD based models on the

other hand are therefore very welcome. The QCD sum rule method [2,3] provides such a link. Before we sketch its basic concepts, however, we want to dwell for a moment on the in-medium properties of hadrons.

For temperatures and densities below but near to the critical values which mark the transition to the QGP it is plausible to expect that already there the properties of the involved hadrons such as, e.g., their masses and decay widths get modified. Especially the aspect of chiral symmetry restoration is interesting here. The properties of chiral partners should start to approach each other and finally become identical in the chirally symmetric phase. Concerning  $\rho$  and  $a_1$  mesons possible scenarios are, e.g., discussed in Refs. [4–6] for the case of finite temperature. In principle one can distinguish three types of possible phenomena (which do not exclude each other).

(a) Mass shifts: The masses of  $\rho$  and  $a_1$  might approach each other. One has to distinguish in which way this actually happens: The masses might meet at a value somewhere in between their vacuum masses (and possibly drop together afterwards). It is, however, also possible that the masses of both mesons drop and finally (approximately) vanish at the point of chiral symmetry restoration.

(b) Peak broadening: From the experimental point of view the  $\rho(a_1)$  meson shows up as a peak in the vector (axial-vector) channel. In a medium the peaks might get broader (maybe without a change of the respective peak positions, i.e., the nominal masses) until the melted spectra in both channels become degenerate.

(c) Mixing: The distinct peaks might maintain (maybe without shifts or broadening), but the  $a_1$  peak shows up with increasing height in the vector channel and vice versa.

In any case, the spectra in the vector and axial-vector channel become degenerate when chiral symmetry becomes restored.

In fact, the  $\rho$  meson is supposed to be a good candidate to search for a sign of chiral symmetry restoration. The reason is that it has the quantum numbers of the photon. Therefore the  $\rho$  meson can decay via a virtual photon into a dilepton pair. If this decay happens within a hot and dense medium the dileptons contain information about the in-medium properties of the  $\rho$  meson. Therefore, in principle the possible scenarios discussed above or a mixture of them should leave their marks in the dilepton spectra. Indeed, the HELIOS and

CERES Collaborations have reported medium modifications in the dilepton spectra in the invariant mass range around the  $\rho$  meson mass [7,8]. Whether the observed spectra can be explained within a conventional hadronic scenario [9] or whether one has to include medium modifications induced by chiral symmetry restoration [10,11] is still a matter of discussion (see, also Refs. [12,13], and references therein). Also for the study of possible in-medium changes of hadronic properties a closer connection between hadrons and QCD is desirable.

The QCD sum rule approach has the merit to relate certain low-energy quantities—which so far are not directly accessible by QCD—with high-energy expressions which can be calculated by the operator product expansion [14] in terms of quark and gluon degrees of freedom. Nonperturbative effects are encoded in the appearance of various quark and gluon condensates. In the following this method is applied to vector and axial-vector mesons placed in a cold medium with finite nuclear density. To clearly work out the modifications when changing from vacuum to a medium we also discuss the vacuum sum rule analysis for  $\rho$  and  $a_1$  in some detail. Before sketching the basic ideas of the sum rule approach we review the present status of in-medium analyses for vector and axial-vector mesons especially in the light of the possible scenarios of in-medium changes discussed above. Concerning finite temperature  $T$  it has been shown [4] that at  $O(T^2)$  and neglecting the pion mass only mixing occurs. A systematic study beyond this linear (pion) density approximation is complicated by unknown nonscalar higher twist condensates [15–17]. For finite nucleon density previous analyses have restricted their attention to the vector channel. In the first analyses [18,19] only a possible mass shift for the  $\rho$  meson has been taken into account, i.e., the possible scenarios of peak broadening and/or mixing as mentioned above have been excluded by hand. In this case it was found that the  $\rho$  meson mass would drop in a nuclear medium. However, it has been shown by the authors of Ref. [20] that their specific hadronic model also fulfills the sum rule (see, also Refs. [21,22]). This model predicts peak broadening for the  $\rho$  meson and basically no mass shift. Subsequently, a systematic study revealed that independently of the chosen hadronic model the sum rule for the  $\rho$  meson for finite density is in accordance with a specific mass-width correlation [23]: For low width the mass has to decrease. If, however, the mass stays constant—or even rises—the width has to increase. The sum rule does not have enough predictive power to fix both the mass and the width of the vector meson. We will come back to that point below. To the best of our knowledge, the third possible in-medium modification, the mixing phenomena, has not yet been included in a systematic sum rule analysis for the vector axial-vector system for finite density. The purpose of the present work is to treat the properties of  $\rho$  and  $a_1$  on equal footing, allowing for mass shifts, peak broadening, and mixing.

Before we turn to the specific sum rule analysis for the chiral partners  $\rho$  and  $a_1$  we discuss some important aspects of the QCD sum rule approach focusing especially on in-medium situations. Recall that our basic motivation was to describe various spectra of heavy-ion collisions by hadronic

models in absence of a QCD description based on first principles. Even when only hadronic models are capable of calculating *observable* quantities one can imagine that it is possible to find other quantities which can be reliably determined both within the hadronic framework and in terms of quark and gluon degrees of freedom. In this way one obtains predictions for hadronic parameters such as masses and coupling constants or cross-check for hadronic models. Concerning the QCD sum rule method such quantities are specific correlators (see below) calculated in the deep space-like region, i.e., for large momenta  $q$  with  $q^2 \ll 0$ . For very large  $Q^2 = -q^2$  QCD perturbation theory becomes applicable. Proceeding to (somewhat) smaller values of  $Q^2$  nonperturbative corrections appear. They can be expanded in a power series in  $1/Q^2$ , called the operator product expansion (OPE):

$$\sum \frac{c_n}{Q^{2n}}. \quad (1.1)$$

In the coefficients  $c_n$  the famous quark and gluon condensates enter. One can imagine the series (1.1) as a separation of the hard (denominator) and soft (numerator) scales of the problem (see, e.g., Ref. [24], and references therein). In the numerator the nonperturbative effects enter. In practice, only the first few coefficients in Eq. (1.1) can be determined. Of course, this does not matter as long as  $Q^2$  is large enough. Thus, the crucial question is for which values of  $Q^2$  one can trust the truncated series. If we want to learn something about a hadron with mass  $m_h$  it turns out that  $Q^2$  has to be of the order of  $m_h^2$ . To get an order of magnitude estimate for the coefficients  $c_n$  we have to ask about the typical scales for nonperturbative effects. Let us discuss step by step the different cases of vacuum, finite temperature and finite baryon density. For vacuum the typical scales are  $\Lambda_{\text{QCD}}$  and the current quark masses. The up and down quark masses have only a few MeV and are therefore negligibly small. The strange quark mass and  $\Lambda_{\text{QCD}}$  are between 100 and 200 MeV. On the other hand, the typical hadron masses are of the order of 1 GeV. Therefore, one might expect that the sum rule analysis leads to reasonable results.<sup>1</sup> Of course, the masses of the much lighter pions and kaons cannot be determined. Unfortunately this optimistic picture is not completely true. In fact, there might be nonperturbative effects which introduce an additional hard scale, such as, e.g., instantons [25]. In this case the series (1.1) would break down for the interesting values of  $Q^2$ . It seems, however, that the influence of such effects on the  $\rho$  and  $a_1$  sum rules is not important. We therefore *assume* throughout this work that the OPE works for the vector and axial-vector channel. Nonetheless, this consideration shows that at present the QCD sum rule approach cannot be directly justified from QCD without any additional assumptions. Therefore it should merely be regarded as a

<sup>1</sup>We restrict our considerations here to hadrons made out of light quarks. The masses of the heavy quarks have to be regarded as part of the hard scale [2].

QCD based model and not as QCD itself. Turning to the case of finite temperature involves new scales. It is common practice to approximate the low-temperature<sup>2</sup> medium by a pion gas. Therefore the new scales are the temperature and the pion mass. Also these quantities are of the order of  $\Lambda_{\text{QCD}}$ . Of course,  $T$  might also be lower. Therefore the previous considerations apply also here. The case of finite baryon density  $\rho_N$  is more complicated. Here one approximates the medium by a Fermi gas of nucleons. New in-medium scales are the Fermi momentum and the nucleon mass. While the former is reasonably small, e.g., for saturation density of nuclear matter, the latter is of the order of 1 GeV. Since the nucleon mass enters the series (1.1) in the numerator it becomes questionable whether the OPE still works (see also the discussion in Ref. [26] and the successive comments [27,28]). Full clarification of this question requires the determination of all coefficients  $c_n$  which would be equivalent to solving QCD in the nonperturbative low-energy domain. This is of course out of reach. For our case at hand there is, however, a class of contributions to the OPE which can be determined to all orders, namely, the twist-two condensates [18,19,24,29]. In fact their contribution to the coefficients in the low density approximation is given by

$$c_n^{\text{twist-two}} = a_n m_N^{2n-3} \rho_N, \quad (1.2)$$

i.e., powers of  $Q^2$  in the denominator which in an optimal situation should suppress higher order contributions in Eq. (1.1) are compensated by powers of  $m_N^2$  in the numerator. Thus the class of twist-two contributions shows exactly the unpleasant feature discussed above. In Eq. (1.2) the dimensionless quantities  $a_n$  can be determined from the parton distributions in a nucleon [18,19,24,29]. Fortunately it turns out that  $a_n$  is strongly decreasing with increasing  $n$  such that the higher dimensional contributions of the twist-two condensates can safely be neglected [24,29]. This is a hint that the OPE still works in the case of finite nuclear density. Of course this is not a proof for the validity of the OPE. Throughout this work we *assume* that the OPE works. In spite of these obvious problems inherent to the QCD sum rule approach for finite density we regard the analysis presented in the following as useful in view of the possibility to learn something about the in-medium properties of hadrons from an approach which deals with the fundamental degrees of freedom of QCD. Nonetheless we stress again that the QCD sum rule approach—especially for the case of finite nuclear density—is not as fundamental as QCD.

This paper is organized in the following way. In the next section we derive the in-medium Borel sum rules for  $\rho$  and  $a_1$  which we will use throughout this work for any quantitative statements. In Sec. III we make a detour to discuss a different type of sum rule, namely, the finite energy sum rule. This will yield a qualitative picture what one has to expect from a sum rule analysis and how much information

one can get. In Sec. IV we introduce our hadronic parametrizations which are used to analyze the sum rules. Results for  $\rho$  and  $a_1$  in vacuum are presented in Sec. V. These results serve as a reference frame with which we can compare the succeeding in-medium results. Section VI is devoted to the discussion of the mixing phenomena while the in-medium results are presented in Sec. VII. Finally we summarize and discuss our results in Sec. VIII.

## II. THE CURRENT-CURRENT CORRELATOR AND THE BOREL SUM RULE

The relevant quantity to look at is the covariant time ordered current-current correlator

$$\Pi_{\mu\nu}(q) = i \int d^4x e^{iqx} \langle T j_\mu(x) j_\nu(0) \rangle. \quad (2.1)$$

For the  $\rho$  meson channel  $j_\mu$  is the isospin-1 part of the electromagnetic current

$$j_\mu^V = \frac{1}{2} (\bar{u} \gamma_\mu u - \bar{d} \gamma_\mu d). \quad (2.2)$$

This current-current correlator enters, e.g., the cross section of  $e^+ e^- \rightarrow$  hadrons (see below). For the  $a_1$  meson channel we have to deal with the corresponding axial-vector current

$$j_\mu^A = \frac{1}{2} (\bar{u} \gamma_\mu \gamma_5 u - \bar{d} \gamma_\mu \gamma_5 d). \quad (2.3)$$

The expectation value in Eq. (2.1) is taken with respect to the surrounding environment. We study here, first, vacuum and, second, an (isospin neutral) equilibrated homogeneous medium with finite nuclear density and vanishing temperature. In the medium Lorentz invariance is broken. All the formulas which we will present in the following refer to the Lorentz frame where the medium is at rest, i.e., where the spatial components of the baryonic current vanish. For simplicity we restrict our considerations to mesons which are at rest with respect to the medium. For the vacuum case we can choose the rest system of the (axial-)vector meson without any loss of generality.

In the following the formulas without an explicit  $V$  or  $A$  index are valid for both vector and axial-vector channel. The correlator (2.1) has the following decomposition (valid for mesons at rest):

$$\Pi_{\mu\nu}(q) = q_\mu q_\nu R(q^2) - g_{\mu\nu} \Pi^{\text{isotr}}(q^2). \quad (2.4)$$

In the following we concentrate on  $R(q^2)$ . In the vector channel one has  $\Pi^{\text{isotr}}(q^2) = q^2 R(q^2)$  since the current  $j_\mu^V$  is conserved. We prefer the use of  $R$  instead of  $\Pi^{\text{isotr}}$  since it has been shown in Refs. [19,30,31] that the Borel sum rule (see below) is rather unstable for the latter quantity. The divergence of the axial-vector channel is solely determined by the pion decay. Hence we would not learn anything new about the  $a_1$  by studying  $\Pi^{\text{isotr}}$  in addition to  $R$ .

Concerning, e.g., the dilepton production one is interested in the values of the dimensionless quantity  $R_V(q^2)$  in the

<sup>2</sup>At high temperatures it is not reasonable to deal with hadronic degrees of freedom. If one wants to learn something about hadrons low temperature expansions are appropriate.

timelike region  $q^2 > 0$ . The reason is that  $R_V$  is related to the cross section  $e^+e^- \rightarrow \text{hadrons}$  with isospin 1 via [32]

$$\frac{\sigma^{I=1}(e^+e^- \rightarrow \text{hadrons})}{\sigma(e^+e^- \rightarrow \mu^+\mu^-)} = 12\pi \text{Im}R_V. \quad (2.5)$$

At least for low energies the timelike region is determined by hadronic degrees of freedom. In principle, there are two possibilities to describe the current-current correlator. First, guided by an educated guess one might use a simple parametrization with some free parameters. Second, one might use a hadronic model, e.g., for vector mesons [13,20,21,33–39] using one or the other form of vector meson dominance. In the following we will explore the first possibility and figure out which constraints for these free parameters are provided by the QCD sum rule approach. For the  $a_1$  we proceed completely analogously. We denote the result for  $R$  in the timelike region by  $R^{\text{had}}$ . On the other hand, the current-current correlator (2.1) can be calculated for  $q^2 \ll 0$  using Wilson's operator product expansion (OPE) [14] for quark and gluonic degrees of freedom [2] (for in-medium calculations see, e.g., Refs. [18,19]). In the following we shall call the result of that calculation  $R^{\text{OPE}}$ . A second representation in the spacelike region which has to match  $R^{\text{OPE}}$  can be obtained from  $R^{\text{had}}$  by utilizing a subtracted dispersion relation. We find

$$R^{\text{OPE}}(Q^2) = \frac{\tilde{c}_1}{Q^2} + \tilde{c}_2 - \frac{Q^2}{\pi} \int_0^\infty ds \frac{\text{Im}R^{\text{had}}(s)}{(s+Q^2)s} \quad (2.6)$$

with  $Q^2 := -q^2 \gg 0$  and some subtraction constants  $\tilde{c}_i$ .

Equation (2.6) connects hadronic with quark-gluon based expressions. In principle, for a given hadronic parametrization of  $R^{\text{had}}$  with free parameters this equation could be used to extract information about these parameters. This, however, would require the knowledge of  $R^{\text{had}}(s)$  for arbitrary large  $s$ . In practice, the situation is such that one has a parametrization for the current-current correlator for the energy region of the lowest hadronic resonance, but one usually has no model which remains valid for arbitrary high energies. In the dispersion integral of Eq. (2.6) higher lying resonances are suppressed, but only by a factor  $1/s^2$ . Clearly, it is desirable to achieve a larger suppression of the part of the hadronic spectral distribution on which one has less access. To this aim, a Borel transformation [2,32] can be applied to Eq. (2.6). For an arbitrary function  $f(Q^2)$  the Borel transformation is defined as

$$f(Q^2) \xrightarrow{\hat{B}} \tilde{f}(M^2) \quad (2.7)$$

with

$$\hat{B} := \lim_{\substack{Q^2 \rightarrow \infty, N \rightarrow \infty \\ Q^2/N = :M^2 = \text{fixed}}} \frac{1}{\Gamma(N)} (-Q^2)^N \left( \frac{d}{dQ^2} \right)^N, \quad (2.8)$$

where  $M$  is the so-called Borel mass. Applying the Borel transformation to Eq. (2.6) we finally get [24]

$$\tilde{R}^{\text{OPE}}(M^2) = \frac{\tilde{c}_1}{M^2} + \frac{1}{\pi M^2} \int_{0^+}^\infty ds \text{Im}R^{\text{had}}(s) e^{-s/M^2}. \quad (2.9)$$

We observe that higher resonance states are now exponentially suppressed. Note that the subtraction constant  $\tilde{c}_2$  of Eq. (2.6) has dropped out. The other one,  $\tilde{c}_1$ , vanishes in vacuum. In a nuclear medium for a meson at rest, we incorporate the Landau damping term in the subtraction constant  $\tilde{c}_1$ . This term comes from the absorption of a spacelike meson by an on-shell nucleon. Having incorporated this term in  $\tilde{c}_1$  we avoid double counting by restricting the integration in Eq. (2.9) to the timelike region. For a detailed discussion of that point see Ref. [40]. One gets in the linear density approximation

$$\tilde{c}_1 = \frac{\rho_N}{4m_N}. \quad (2.10)$$

Equation (2.9) is the QCD sum rule which we will utilize in the following.

Having achieved a reasonable suppression of the energy region above the lowest lying resonance the integral in Eq. (2.9) is no longer sensitive to the details of the hadronic spectral distribution in that region. For high energies the quark structure of the current-current correlator is resolved. QCD perturbation theory becomes applicable yielding

$$\text{Im}R^{\text{had}}(s) = \frac{1}{8\pi} \left( 1 + \frac{\alpha_s}{\pi} \right) \quad \text{for large } s. \quad (2.11)$$

These considerations suggest the ansatz

$$\text{Im}R^{\text{had}}(s) = \Theta(s_0 - s) \text{Im}R^{\text{res}}(s) + \Theta(s - s_0) \frac{1}{8\pi} \left( 1 + \frac{\alpha_s}{\pi} \right), \quad (2.12)$$

where  $s_0$  denotes the threshold between the low energy region described by a spectral function for the lowest lying resonance  $\text{Im}R^{\text{res}}$ , and the high-energy region described by a continuum calculated from perturbative QCD. In the following we use  $\alpha_s(1 \text{ GeV}) \approx 0.36$ . Of course, the high-energy behavior given in Eq. (2.12) is only an approximation on the true spectral distribution for the current-current correlator. Also the rapid crossover in Eq. (2.12) from the resonance to the continuum region is not realistic. However, exactly here the suppression factors discussed above should become effective making a more detailed description of the crossover and the high-energy region insignificant. The price we have to pay for the simple decomposition (2.12) is the appearance of a new parameter  $s_0$ , the continuum threshold, which in general depends on the nuclear density. We will elaborate below on the determination of  $s_0$ .

To study the content of Eq. (2.9) for the vector and axial-vector channel we need the OPE for the left-hand side (LHS). In general, it is given by a Taylor expansion in  $1/M^2$ :

$$\tilde{R}^{\text{OPE}}(M^2) = \sum \frac{c_n}{M^{2n}}. \quad (2.13)$$

In the following we present the formulas for the case of finite nuclear density  $\rho_N$ . The vacuum case [2] is easily obtained by  $\rho_N \rightarrow 0$ . For the vector channel one gets [18,19] (for details see also Ref. [24], and references therein)

$$c_0^V = \frac{1}{8\pi^2} \left( 1 + \frac{\alpha_s}{\pi} \right), \quad (2.14a)$$

$$c_1^V = 0, \quad (2.14b)$$

$$c_2^V = \frac{1}{24} \left\langle \frac{\alpha_s}{\pi} G^2 \right\rangle + \frac{1}{4} m_N A_2 \rho_N + m_q \langle \bar{q}q \rangle, \quad (2.14c)$$

$$c_3^V = -\frac{5}{24} m_N^3 A_4 \rho_N - \frac{56}{81} \pi \alpha_s \langle \mathcal{O}_4^V \rangle \quad (2.14d)$$

while for the axial-vector sector one obtains [2,15]

$$c_i^A = c_i^V \quad \text{for } i=0,1,2, \quad (2.15a)$$

$$c_3^A = -\frac{5}{24} m_N^3 A_4 \rho_N + \frac{88}{81} \pi \alpha_s \langle \mathcal{O}_4^A \rangle. \quad (2.15b)$$

We neglect (unknown) condensates with dimension higher than 6 and some less important twist-4 condensates and  $\alpha_s$  corrections (see Refs. [19,41,24]). We also neglect perturbative contributions proportional to the square of the current quark masses. Note that all expectation values have to be taken with respect to the medium. We work here in the linear density approximation

$$\langle \mathcal{O} \rangle \approx \langle \mathcal{O} \rangle_{\text{vac}} + \frac{\rho_N}{2m_N} \langle N | \mathcal{O} | N \rangle. \quad (2.16)$$

A single nucleon state is denoted by  $|N\rangle$ . It is normalized according to

$$\langle N(\vec{k}) | N(\vec{k}') \rangle = (2\pi)^3 2E_k \delta(\vec{k} - \vec{k}'). \quad (2.17)$$

We defer the calculation of the in-medium expectation values of the scalar operators to Sec. VI and only discuss their vacuum expectation values here. For the gluon condensate we use a canonical value of [2]  $\langle (\alpha_s/\pi) G^2 \rangle_{\text{vac}} = (330 \text{ MeV})^4$ . As compared to the gluon-condensate the influence of the two-quark condensate [2]

$$m_q \langle \bar{q}q \rangle_{\text{vac}} = -\frac{1}{2} f_\pi^2 m_\pi^2 \quad (2.18)$$

is rather small (and is further diminished in a nuclear environment). Here  $f_\pi = 93 \text{ MeV}$  denotes the pion decay constant and  $m_\pi$  the pion mass. While the values for gluon and two-quark condensate are fairly well known the knowledge about the four-quark condensates<sup>3</sup>

<sup>3</sup>Note that the definition of  $\langle \mathcal{O}_4^{V/A} \rangle$  is chosen such that the factorization assumption would imply  $\langle \mathcal{O}_4^{V/A} \rangle \approx \langle \bar{q}q \rangle^2$ .

$$\begin{aligned} \langle \mathcal{O}_4^V \rangle &= \frac{81}{224} \langle (\bar{u} \gamma_\mu \gamma_5 \lambda^a u - \bar{d} \gamma_\mu \gamma_5 \lambda^a d)^2 \rangle \\ &+ \frac{9}{112} \left\langle (\bar{u} \gamma_\mu \lambda^a u + \bar{d} \gamma_\mu \lambda^a d) \sum_{\psi=u,d,s} \bar{\psi} \gamma^\mu \lambda^a \psi \right\rangle \end{aligned} \quad (2.19)$$

and

$$\begin{aligned} \langle \mathcal{O}_4^A \rangle &= -\frac{81}{352} \langle (\bar{u} \gamma_\mu \lambda^a u - \bar{d} \gamma_\mu \lambda^a d)^2 \rangle \\ &- \frac{9}{176} \left\langle (\bar{u} \gamma_\mu \lambda^a u + \bar{d} \gamma_\mu \lambda^a d) \sum_{\psi=u,d,s} \bar{\psi} \gamma^\mu \lambda^a \psi \right\rangle \end{aligned} \quad (2.20)$$

is very limited. Traditionally factorization is assumed which, however, probably underestimates its value. In the following we will use two values for the four-quark condensates to explore the sensitivity of the results

$$\langle \mathcal{O}_4^V \rangle_{\text{vac}}, \langle \mathcal{O}_4^A \rangle_{\text{vac}} = (-292 \text{ MeV})^6, (-281 \text{ MeV})^6. \quad (2.21)$$

The larger value is chosen as to obtain an optimal agreement between QCD sum rule prediction and experiment for the  $\rho$  meson properties in vacuum. Finally the terms proportional to  $A_2$  and  $A_4$  in Eqs. (2.14), (2.15) stem from twist-2 condensates. They are obtained from the moments of the quark distributions in a nucleon [18]. We use  $A_2 = 0.9$ ,  $A_4 = 0.12$ .

So far we have not specified for which values of  $M^2$  we regard the sum rule (2.9) to be valid. Note that in practice Eq. (2.13) is a truncated series in  $1/M^2$ . Clearly, if  $M^2$  is too small the  $1/M^2$  expansion in Eq. (2.13) breaks down. On the other hand, however, if  $M^2$  is too large the exponential in Eq. (2.9) does not sufficiently suppress the intermediate- and high-energy parts of  $\text{Im}R^{\text{had}}(s)$  given in Eq. (2.12). As mentioned above this suppression is important since the modeling of the region around the threshold  $s_0$  is rather crude. If these qualitative considerations are put on a more quantitative level one can define a so called Borel window for the masses  $M^2$  in which the sum rule is valid (see, e.g., Ref. [23]). Following Ref. [30] we determine the minimal Borel mass such that the last accessible contribution to the OPE (2.13), i.e., here the  $1/M^6$  term, amounts to 10% of the total OPE result

$$\left| \frac{c_3}{M_{\text{min}}^6} \right| = 0.1 \tilde{R}^{\text{OPE}}(M_{\text{min}}^2). \quad (2.22)$$

The maximal Borel mass is chosen such that the continuum contribution to the right-hand side (RHS) of Eq. (2.9) does not become larger than the contribution from the resonance which we want to study, i.e.,

$$\begin{aligned} \int_0^\infty ds \frac{1}{8\pi} \left( 1 + \frac{\alpha_s}{\pi} \right) \Theta(s - s_0) e^{-s/M_{\text{max}}^2} \\ = \int_0^\infty ds \text{Im}R^{\text{res}}(s) \Theta(s_0 - s) e^{-s/M_{\text{max}}^2}. \end{aligned} \quad (2.23)$$

As a guideline one can expect that  $M_{\max}^2$  scales with the point where the average strength of  $\text{Im}R^{\text{res}}(s)$  is located, i.e., with the resonance mass (squared). Hence for large (small) resonance masses the value of  $M_{\max}^2$  will be large (small). It might appear that in some cases the Borel window between  $M_{\min}^2$  and  $M_{\max}^2$  is rather small or even closed. Then the sum rule is meaningless. In practice the determination of the Borel window provides a quality check for the sum rule.

### III. FINITE ENERGY SUM RULES—THE QUALITATIVE PICTURE

The Borel sum rule (2.9) is not the only sum rule which is used to connect hadronic and QCD based information. Inserting Eq. (2.12) in Eq. (2.9) and expanding the RHS in powers of  $1/M^2$  one can compare the coefficients of this expansion with the respective ones in the series on the LHS given by Eq. (2.13). This yields the finite energy sum rules<sup>4</sup> (presented here for the  $\rho$  meson for the vacuum case)

$$\frac{1}{\pi} \int_0^{s_0} ds \text{Im}R_V^{\text{res}}(s) - c_0^V s_0 = 0, \quad (3.1a)$$

$$-\frac{1}{\pi} \int_0^{s_0} ds s \text{Im}R_V^{\text{res}}(s) + c_0^V \frac{s_0^2}{2} = c_2^V, \quad (3.1b)$$

$$\frac{1}{\pi} \int_0^{s_0} ds s^2 \text{Im}R_V^{\text{res}}(s) - c_0^V \frac{s_0^3}{3} = 2c_3^V, \quad (3.1c)$$

where the coefficients of the OPE are given in Eq. (2.14), evaluated in this section for  $\rho_N=0$ .

The first two of these sum rules are utilized, e.g., in Ref. [43]. Obviously the expansion of the RHS of Eq. (2.9) relies on the assumption that the Borel sum rule obtained by the simple decomposition (2.12) is valid for arbitrary high values of  $M^2$ . As pointed out above this is doubtful due to the limited knowledge of  $\text{Im}R^{\text{had}}(s)$  in the threshold region. Actually the sensitivity of the respective finite energy sum rule on the details of  $\text{Im}R^{\text{had}}(s)$  around  $s_0$  is increasing when going from Eq. (3.1a) to Eq. (3.1c). Thus it might be safe to extract information from the lowest finite energy sum rule(s). Utilizing higher ones, however, becomes more and more doubtful. This is the reason why we prefer to use the Borel sum rule. In addition, for the latter one a consistency check on its validity is provided by the determination of the Borel window.<sup>5</sup>

<sup>4</sup>This derivation is actually oversimplified since it neglects the running of the coupling constant. For a rigorous derivation see Ref. [42] and references therein.

<sup>5</sup>A consistency check for finite energy sum rules might be obtained in the following way: Clearly the discontinuity between the resonance and the continuum region in Eq. (2.12) is unrealistic. It is only used to avoid new additional parameters. Introducing instead a smooth crossover one can test the sensitivity of the finite energy sum rules on these new parameters which model the crossover region. If a finite energy sum rule appears to be fairly insensitive to these new parameters it might be regarded as useful.

Nonetheless, the finite energy sum rules can be used to get a qualitative picture about the connection of the OPE side to resonance parameters like mass and width. In fact,  $\text{Im}R_V^{\text{res}}$  is a mass distribution. Therefore it appears natural to define the first two moments of this distribution, i.e., an average mass and a width via

$$\bar{m}^2 := \frac{\int_0^{s_0} ds s \text{Im}R_V^{\text{res}}(s)}{\int_0^{s_0} ds \text{Im}R_V^{\text{res}}(s)} \quad (3.2)$$

and

$$\sigma^2 \bar{m}^2 := \frac{\int_0^{s_0} ds (s - \bar{m}^2)^2 \text{Im}R_V^{\text{res}}(s)}{\int_0^{s_0} ds \text{Im}R_V^{\text{res}}(s)}. \quad (3.3)$$

Obviously, the finite energy sum rules (3.1) can be used to connect these moments with the condensates (and the continuum threshold):

$$\bar{m}^2 = \frac{s_0}{2} - \frac{c_2}{c_0 s_0}, \quad (3.4)$$

$$\sigma^2 = \frac{1}{\bar{m}^2} \left( \frac{s_0^2}{3} + \frac{2c_3}{c_0 s_0} - \bar{m}^4 \right). \quad (3.5)$$

We can learn two things from these simple relations: First, the average mass is determined by the dimension-4 (gluon and two-quark) condensates and the continuum threshold while the dimension-6 condensates (here the four-quark condensate) influence only the width. Second, we do not have enough information at hand to determine all the phenomenological parameters. In our case at hand we have three of them, namely the continuum threshold  $s_0$  and the two moments  $\bar{m}^2$  and  $\sigma^2$ . On the other hand, we only have two equations for these parameters. Traditionally, the use of QCD sum rules is accompanied by an additional assumption, namely that the width is negligible. In this case the mass can be determined. In general, however, the best we can hope to gain are correlations between the free parameters. Being especially interested in mass and width we can vary  $s_0$  and determine the corresponding values for  $\bar{m}$  and  $\sigma$ . The result is shown in Fig. 1. [For the four-quark condensate (2.21) we have chosen the larger value.] The most important thing to note here is that the width grows with rising mass. We will find correlations of this kind again and again throughout this work. The qualitative understanding of this correlation is obtained from the simple relations (3.4), (3.5). We are reluctant, however, to draw any quantitative conclusions from the previous considerations. In principle we are interested in the properties of the vector and axial-vector resonances, e.g., their masses and widths as defined via Breit-Wigner-type parametrizations. In general, these masses and widths are *not*

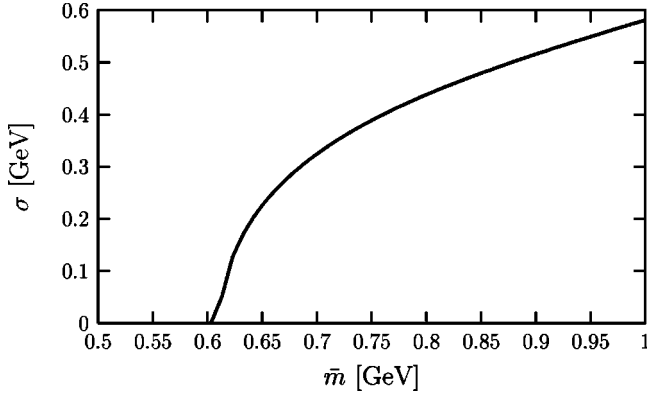


FIG. 1. Correlation between mass  $\bar{m}$  and width  $\sigma$  for the  $\rho$  meson as obtained from the finite energy sum rules (3.4), (3.5). See text for details.

identical to the moments  $\bar{m}^2$  and  $\sigma^2$  of the distribution  $\text{Im}R^{\text{res}}$ . In addition, as outlined above we doubt the quantitative reliability of the finite energy sum rules (3.1) due to their higher sensitivity to the details of the high-energy behavior. Hence we prefer the use of the Borel sum rule (2.9). For a very elaborate use of combinations of finite energy sum rules we refer to Ref. [42].

#### IV. BREIT-WIGNER PARAMETRIZATION OF THE CURRENT-CURRENT CORRELATOR

The only remaining question is how to parametrize  $\text{Im}R^{\text{res}}(s)$  which enters the sum rule (2.9) via Eq. (2.12). Concerning the vector channel, experiments which determine, e.g.,  $e^+e^- \rightarrow \pi^+\pi^-$  suggest the parametrization

$$\text{Im}R_V^{\text{res}}(s) = \pi F_\rho \frac{S_\rho(s)}{s}. \quad (4.1)$$

Here  $F_\rho$  determines the absolute height of the spectrum and  $S_\rho$  denotes the spectral function of the  $\rho$  meson which we will specify further below. Concerning the axial-vector channel not only the  $a_1$  but also the pion shows up there. Hence the parametrization has to be extended to

$$\text{Im}R_A^{\text{res}}(s) = \pi F_{a_1} \frac{S_{a_1}(s)}{s} + \pi f_\pi^2 \delta(s - m_\pi^2). \quad (4.2)$$

The spectral functions are given by

$$S(s) = \frac{1}{\pi} \frac{\sqrt{s}\Gamma(s)}{(s - m^2)^2 + s\Gamma(s)^2}. \quad (4.3)$$

Here  $m$  is the mass of the respective meson and  $\Gamma$  its width. We stress again that these Breit-Wigner parameters are not identical to the moments introduced in the last section; there is only a qualitative correspondence. We denote the on-shell width by

$$\gamma = \Gamma(m^2). \quad (4.4)$$

We have to use an  $s$ -dependent width in Eq. (4.3) for the following reason: In the following we will vary  $\gamma$  (and other parameters) over large ranges. As outlined above the sum rule (2.9) is insensitive to the modeling of the high-energy behavior of  $\text{Im}R^{\text{res}}(s)$ . In turn, there is a high sensitivity to the low-energy part. Therefore, especially for large widths we have to make sure that at threshold the spectral function shows the correct behavior. On the other hand, we do not want to overweight our parametrizations with too many independent parameters. Hence, we are aiming at simple parametrizations which reproduce correctly the threshold behavior.

In the vacuum the width of the  $\rho$  meson is governed by the decay into two pions. We use the following parametrization:

$$\Gamma_\rho^{\text{decay}}(s) = \gamma_\rho \frac{m_\rho^2}{s} \left( \frac{p_{\text{rel}}^{\pi\pi}(s)}{p_{\text{rel}}^{\pi\pi}(m_\rho^2)} \right)^3 \Theta(s - 4m_\pi^2) \quad (4.5)$$

with the momentum of the pions in the rest frame of the decaying  $\rho$  with invariant mass  $\sqrt{s}$ :

$$p_{\text{rel}}^{\pi\pi}(s) = (s - 4m_\pi^2)^{1/2}/2. \quad (4.6)$$

Concerning the  $a_1$  meson in vacuum its width is dominated by the decay into rho plus pion. For simplicity we neglect the width of the rho meson here and use

$$\Gamma_{a_1}^{\text{decay}}(s) = \gamma_{a_1} \frac{m_{a_1}^2}{s} \frac{p_{\text{rel}}^{\pi\rho}(s)}{p_{\text{rel}}^{\pi\rho}(m_{a_1}^2)} \Theta[s - (m_\rho + m_\pi)^2] \quad (4.7)$$

with the momentum of pion and rho in the rest frame of the decaying  $a_1$  with invariant mass  $\sqrt{s}$ :

$$p_{\text{rel}}^{\pi\rho}(s) = \{[s - (m_\rho + m_\pi)^2][s - (m_\rho - m_\pi)^2]\}^{1/2}/(2\sqrt{s}). \quad (4.8)$$

In a nuclear environment a presumably rather sizable collisional width (see Ref. [39], and references therein) has to be added to the decay width. The lowest threshold for a (axial-)vector meson collision with a nucleon is given by the formation of pion plus nucleon. We assume that the threshold behavior is dominated by the lowest accessible partial wave. For the  $\rho$  meson this is an  $s$  wave leading to

$$\Gamma_\rho^{\text{coll}}(s) = \gamma_\rho \left( \frac{1 - m_\pi^2/s}{1 - m_\pi^2/m_\rho^2} \right)^{1/2} \Theta(s - m_\pi^2). \quad (4.9)$$

For the  $a_1$  meson it is a  $p$  wave

$$\Gamma_{a_1}^{\text{coll}}(s) = \gamma_{a_1} \frac{s}{m_{a_1}^2} \left( \frac{1 - m_\pi^2/s}{1 - m_\pi^2/m_{a_1}^2} \right)^{3/2} \Theta(s - m_\pi^2). \quad (4.10)$$

For the vacuum case  $\Gamma_{\rho/a_1}(s)$  in Eq. (4.3) is given by Eqs. (4.5) and (4.7), respectively. For the case of nuclear medium we restrict ourselves to the two extreme possibilities that the width is either dominated by decays or by collisions. Hence

we explore the two cases that  $\Gamma_{\rho/a_1}(s)$  is either given by Eqs. (4.5) and (4.7) or by Eqs. (4.9) and (4.10).

We will treat  $F$ ,  $m$ ,  $\gamma$  and also the continuum threshold  $s_0$  [see Eq. (2.12)] as free parameters. The aim is to find out how the sum rule (2.9) constrains these parameters. As a general rule one can at best determine as many parameters of the hadronic side of the sum rule as one has powers in  $1/M^2$  on the OPE side [19]. For the latter we have given in Eqs. (2.14), (2.15) four orders in powers of  $1/M^2$ . However, the perturbative part [ $(1/M^2)^0$  part] has already been used to determine the high-energy behavior in Eq. (2.12). Therefore at best only three parameters of the hadronic spectral distribution can be determined from the sum rule (2.9).<sup>6</sup> On the other hand, we have for each meson four free parameters in the parametrization (2.12), (4.1)–(4.3). In the traditional sum rule approach [2,18,19,32,41] the width of the respective meson resonance is neglected (narrow width approximation). In this case the number of free parameters reduces to 3 and the sum rule gains predictive power. This, however, means that in addition to the QCD input represented by the OPE one needs further knowledge to extract predictions from QCD sum rules. In vacuum, this additional input comes from experiments which tell us that, e.g., the  $\rho$  meson indeed is a well-defined resonance with a width considerably smaller than the mass. In contrast, for the in-medium case it is so far not clear if the pronounced peak structure of the  $\rho$  meson survives in a nuclear surrounding or if it is washed out [20,35–39], e.g., by its coupling to resonance-hole states. The  $a_1$  meson already has a large vacuum decay width. In addition, its mass is so high that it is hard to achieve a clear separation between  $\text{Im}R^{\text{res}}$  and the high-energy continuum in Eq. (2.12) [2]. We will come back to that point below when discussing the results of our QCD sum rule analysis for the  $a_1$ . As for the  $\rho$  meson, medium effects in addition presumably lead to an additional broadening of the  $a_1$ . To study the influence of the widths of the vector and axial-vector meson on the results extracted from QCD sum rules we will refrain from neglecting  $\gamma$  and proceed with our general parametrization (4.3).

## V. RESULTS FOR VACUUM

We shall now explore which values of mass and width of the  $\rho/a_1$  meson are compatible with the sum rule (2.9). For that purpose we vary the values for  $m$  and  $\gamma$  in large ranges. For a given pair of mass and width we tune the remaining parameters  $F$  and  $s_0$  such that the agreement between left- and right-hand side of Eq. (2.9) is best. The resulting minimal deviation  $d$  between LHS and RHS is a measure for the compatibility of the chosen mass-width pair with the sum rule, i.e., if  $d$  is sufficiently small one might conclude that the chosen pair of mass and width is allowed by QCD sum rules. We regard the sum rule to be approximately valid in the

<sup>6</sup>This is also true if the finite energy sum rules were used instead of the Borel sum rule. The three sum rules (3.1) provide three constraints on the hadronic spectral distribution. See also the discussion in Sec. III.

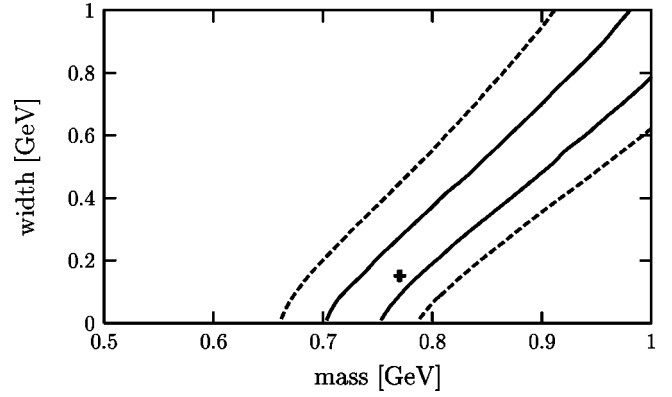


FIG. 2. Deviation  $d$  as a function of width and mass of the  $\rho$  meson for vacuum. For the four-quark condensate a value of  $(-292 \text{ MeV})^6$  has been used. The full lines border the region of QCD sum rule allowed parameter pairs with  $d \leq 0.2\%$ , the dashed lines border the allowed region for  $d \leq 0.5\%$ . The cross marks the experimental values for mass and width of the  $\rho$  meson [including the (very small) error bars according to Ref. [50]].

range given by the Borel window introduced above. Hence we define the deviation  $d$  as an average over this window (see Ref. [23] for further details).

For the  $\rho$  meson Figs. 2 and 3 show the allowed ranges for mass and width for the vacuum case for the two different values of the four-quark condensate given in Eq. (2.21). Obviously, there is not only one point where the sum rules is reasonably fulfilled but a whole band of allowed mass-width pairs. Figures 2 and 3 qualitatively resemble Fig. 1: the band of allowed mass-width pairs describes a correlation where the width rises with rising mass. Quantitatively, however, the differences between Fig. 1 and Figs. 2,3 are large stressing again that the distribution moments defined in Sec. III are not identical to mass and on-shell width of the Breit-Wigner type spectral functions (4.3). We have also included the experimental point for the  $\rho$  meson in Figs. 2 and 3. Obviously the value of  $(-292 \text{ MeV})^6$  provides an optimal choice for the four-quark condensate. A smaller value for that condensate shifts the band of allowed mass-width pairs either upwards or to the left (or both). From our qualitative considerations of Sec. III we expect that the four-quark condensate mainly

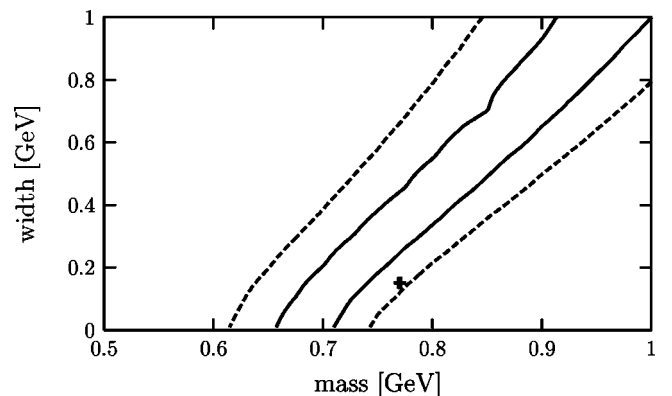


FIG. 3. Same as Fig. 2 but with a four-quark condensate of  $(-281 \text{ MeV})^6$ .



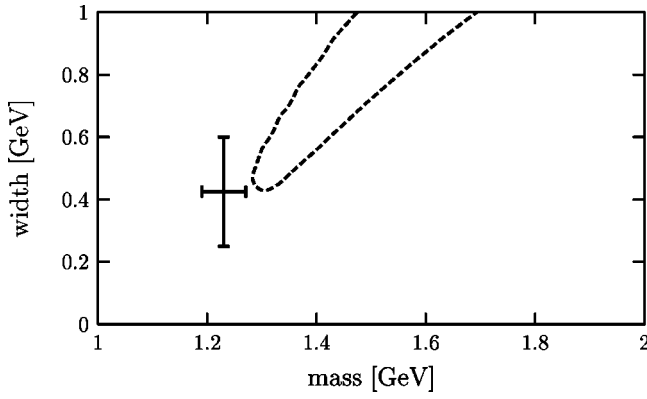


FIG. 4. Same as Fig. 2 for  $a_1$  meson in vacuum; value for four-quark condensate:  $(-292 \text{ MeV})^6$ . The cross marks the experimental values for mass and width of the  $a_1$  meson (including the error bars according to Ref. [50]).

influences the width [see Eq. (3.5)]. Hence a smaller value of the four-quark condensate is supposed to increase the width,<sup>7</sup> i.e., to shift the band upwards. We will further clarify that point when discussing the results for the  $a_1$  meson. Note that also for the smaller value of the four-quark condensate of  $(-281 \text{ MeV})^6$  the deviation  $d$  is still reasonably small for the experimental point (0.46%). As discussed above the results of Figs. 2 and 3 are only meaningful if the Borel window is reasonably large. For our choice for the condensate values leading to Fig. 2 we get  $M_{\min}^2 = 0.71 \text{ GeV}^2$ . The value for  $M_{\max}^2$  depends on the resonance parameters. As already mentioned small values for the resonance mass lead to small values for  $M_{\max}^2$ . For the case at hand we find  $M_{\max}^2 > 1.5 \text{ GeV}^2$  for all mass-width pairs lying in the inner band shown in Fig. 2 and to the right of it. We regard that as a reasonably large Borel window. For Fig. 3 the corresponding values are  $M_{\min}^2 = 0.65 \text{ GeV}^2$  and  $M_{\max}^2 > 1.4 \text{ GeV}^2$ .

Concerning the  $a_1$  meson the corresponding mass-width correlations are shown in Figs. 4 and 5. Qualitatively we find again the same correlation between masses and widths. However, a tendency is visible that the sum rule supports large values of the width. We will find that this tendency increases for the in-medium case. Comparing Figs. 4 and 5 we find that a decrease in the four-quark condensate shifts the band to some extent to the left but merely downwards. To understand that finding we note that the four-quark condensate enters with a different sign in the two sum rules for  $\rho$  and  $a_1$ , respectively; see Eqs. (2.14d), (2.15b). Therefore we expect an upward shift with decreasing four-quark condensate for the  $\rho$  meson, as discussed above, and a downward shift for the  $a_1$ . Figures 4 and 5 support our considerations. Comparing the results with the experimental values for mass and width of the  $a_1$  meson we find that the smaller value for the four-quark condensate (Fig. 5) appears to be much better suited—quite opposite to the case of the  $\rho$  meson where the larger value provides a better fit. In principle, there is no

<sup>7</sup>Note that the four-quark condensate enters the sum rule for the  $\rho$  meson with a negative sign, cf. Eq. (2.14d).

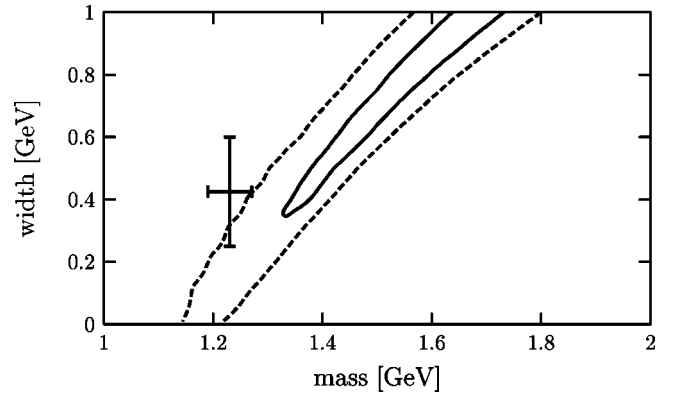


FIG. 5. Same as Fig. 2 for  $a_1$  meson in vacuum; value for four-quark condensate:  $(-281 \text{ MeV})^6$ . The cross marks the experimental values for mass and width of the  $a_1$  meson (including the error bars according to Ref. [50]).

fundamental reason why the four-quark condensates for  $\rho$  and  $a_1$  should be exactly the same. Only if the factorization assumption strictly holds the two quantities defined in Eqs. (2.19) and (2.20) coincide. Still, however, the values  $(-292 \text{ MeV})^6$  and  $(-281 \text{ MeV})^6$  are rather close. For the succeeding in-medium calculations we will choose the respective better value, i.e.,  $(-292 \text{ MeV})^6$  for the  $\rho$  meson and  $(-281 \text{ MeV})^6$  for the  $a_1$ . We note that for the  $a_1$  vacuum case a further reduction of the four-quark condensate does not improve the agreement between the sum rule and the experimental results as the band is further shifted downwards and not to the left. Hence the agreement between sum rule and experiment appears to be better for the  $\rho$  than for the  $a_1$  meson. This rather old finding [2] is most likely due to the fact that the separation between the resonance and the continuum region is better realized in the vector channel. If the resonance appears to be closer to the continuum the sum rule is more sensitive to the details of the modeling of the nearby transition to the continuum. Such details are necessarily rather crude in our ansatz (2.12). Finally we present the results for the Borel window for the preferable parameter choice (Fig. 5): We find  $M_{\min}^2 = 0.71 \text{ GeV}^2$  while all mass-width pairs enclosed by the dashed line obey  $M_{\max}^2 > 1.4 \text{ GeV}^2$ . We note that we have not included the pion branch in the determination (2.23) of the maximal Borel mass to make sure that we really learn something about the properties of the  $a_1$  meson.

## VI. IN-MEDIUM CORRELATORS AND $\rho$ - $A_1$ MIXING

Next we turn to the case of finite nuclear density. As pointed out by several groups (e.g., Refs. [44,45]) the interaction of the  $\rho$  meson with the pion cloud of the nucleons induces a mixing of the  $\rho$  with its chiral partner the  $a_1$  meson. This means that, e.g., the (possibly medium-modified)  $a_1$  peak shows up in the spectral distribution  $\text{Im}R_V^{\text{had}}$  of the vector correlator and vice versa. Suppose now that one would ignore that multippeak structure and still parametrize  $\text{Im}R_V^{\text{had}}$  with only one peak according to Eqs. (2.12), (4.1). In a QCD sum rule analysis one has only access on certain mass

averages of the spectral distribution on account of Eq. (2.9). Hence with a one-peak structure ansatz one would translate certain in-medium changes of the OPE side to changes of mass and width of this peak which in reality, however, are caused by the appearance of other distinct peaks. This would be rather misleading. Indeed, for the comparable case of finite temperature  $T$  it has been shown [4] that the masses of  $\rho$  and  $a_1$ , if understood as the positions of peaks in spectral distributions, do not change in the linear (pion) density approximation.<sup>8</sup> Only if the notion of mass is used with a different meaning (e.g., in the spirit of Sec. III as the first moment of a spectral distribution) it would be correct to attribute an in-medium  $O(T^2)$  mass shift to this ‘‘mass.’’ For considerations beyond the  $O(T^2)$  approximation we refer to Refs. [16,17].

Concerning the present work the mass  $m$  of a resonance (which shows up in the spectral distribution of the current correlator) is defined via Eq. (4.3). For small width it gives the peak position of the resonance. In the following for our case of finite nucleon density we also try to account for the multipeak structures caused by mixing of vector and axial-vector currents. If we only used the sum rule (2.9) and introduced more than one peak, e.g., in Ref. (4.1) we would have too many free parameters to draw any meaningful conclusion. Therefore (as for the case of finite temperature [4]) the key idea is to isolate the contribution of the respective new in-medium peak(s) also for the OPE side. In this way one obtains sum rules for nonmixed correlators (in the following called ‘‘bare’’) which can be analyzed with the one-peak ansatz (plus continuum, of course). These (in general unobservable) bare correlators mix to yield finally the ‘‘full’’ in-medium correlators. The imaginary part of the latter in principle can be observed [see, e.g., Eq. (2.5)]. We note that for the case of finite temperature the bare correlators coincide with the vacuum correlators in the linear density approximation [4]. As we shall see in the following, things are not so simple for the case of finite nucleon density.

To account for the interaction of the nuclear pions with the vector- and axial-vector currents nuclear matter is separated into a Fermi gas of bare nucleons plus soft pions, schematically [44]

$$|\Psi\rangle = \Psi^A|A\rangle + \sum_a \Psi_a^A|A\pi_a\rangle + \sum_{a,b} \Psi_{a,b}^A|A\pi_a\pi_b\rangle + \dots, \quad (6.1)$$

where  $|\Psi\rangle$  denotes the full nuclear matter state vector while  $|A\rangle$  denotes the bare one. The current-current correlator (2.1) evaluated with respect to  $|\Psi\rangle$  can now be decomposed into a bare correlator, i.e., a correlator with respect to  $|A\rangle$ , and a part involving the interaction with (soft) pions:

$$\Pi_{\mu\nu} = \Pi_{\mu\nu}^b + \Pi_{\mu\nu}^\pi. \quad (6.2)$$

<sup>8</sup>Note that an  $O(T^2)$  modification at finite temperature corresponds exactly to  $O(\rho_N/m_N)$  at finite baryon density (see, e.g., Eq. (3) in Ref. [4]).

The latter one is approximately evaluated using soft pion techniques (see also Ref. [15]) and taking into account up to two pions in the initial and/or final state. One gets

$$\begin{aligned} & \langle A\pi^a | Tj_\mu(x)j_\nu(0) | A\pi^b \rangle \\ & \simeq \langle A\pi^a\pi^b | Tj_\mu(x)j_\nu(0) | A \rangle \\ & \simeq \langle A | Tj_\mu(x)j_\nu(0) | A\pi^a\pi^b \rangle \\ & \simeq \frac{-1}{f_\pi^2} \langle A | [Q_5^a, [Q_5^b, Tj_\mu(x)j_\nu(0)]] | A \rangle, \end{aligned} \quad (6.3)$$

with the isovector axial charge

$$Q_5^a = \int d^3x \bar{\psi}(x) \gamma_0 \gamma_5 \frac{\tau^a}{2} \psi(x). \quad (6.4)$$

To calculate the commutators in Eq. (6.3) with the currents (2.2) and (2.3) it is useful to generalize the latter to the full isospin multiplets

$$V_\mu^a = \psi \gamma_\mu \tau^a \psi, \quad A_\mu^a = \psi \gamma_\mu \gamma_5 \tau^a \psi. \quad (6.5)$$

In fact, on account of [32]

$$[Q_5^a, V_\mu^b] = i\epsilon^{abc} A_\mu^c, \quad [Q_5^a, A_\mu^b] = i\epsilon^{abc} V_\mu^c, \quad (6.6)$$

the vector and axial-vector currents are mixed by their interaction with the nuclear pions. Finally the expectation values in Eq. (6.3) have to be weighted by the density of pions in the nuclear medium. For the dimensionless quantities defined in Eq. (2.4) one ends up with (see Ref. [44] for details)

$$R_V(q^2) = R_V^b(q^2) - \xi [R_V^b(q^2) - R_A^b(q^2)], \quad (6.7a)$$

$$R_A(q^2) = R_A^b(q^2) - \xi [R_A^b(q^2) - R_V^b(q^2)], \quad (6.7b)$$

where  $R_{V/A}^b$  denotes the respective correlator with respect to a system of *bare* nucleons, i.e., without their pionic cloud. The mixing parameter is given by

$$\xi = \frac{4}{3} \frac{\sigma_N^\pi \rho_N}{f_\pi^2 m_\pi^2}. \quad (6.8)$$

Here we have introduced [45]

$$\sigma_N^\pi = \frac{m_\pi^2}{4m_N} \langle N | \vec{\pi}^2 | N \rangle = \frac{m_\pi}{2} N_\pi, \quad (6.9)$$

where  $N_\pi$  denotes the scalar number of pions in the cloud surrounding the nucleon.  $\sigma_N^\pi$  contributes to the nucleon sigma term  $\sigma_N$  given by [24]

$$\sigma_N = \frac{m_q}{m_N} \langle N | \bar{q}q | N \rangle. \quad (6.10)$$

Having split up the nucleons into bare nucleons plus a cloud of soft pions we have to disentangle the nucleon sigma term correspondingly [45]:

$$\sigma_N = \sigma_N^b + \sigma_N^\pi. \quad (6.11)$$

At present, the value and even the sign for  $\sigma_N^\pi$  is not a settled issue. We take a *positive* value of 25 MeV. This is in agreement with Ref. [45] but in contrast to Ref. [44] where a negative value has been used. Our choice for  $\sigma_N^\pi$  is motivated by the fact that this ensures that the two correlators  $R_V$  and  $R_A$  become degenerate at some finite density:

$$R_V - R_A = (1 - 2\xi)(R_V^b - R_A^b). \quad (6.12)$$

A negative value for  $\sigma_N^\pi$  would lead to antimixing, i.e., in this case the nuclear pions would work against chiral symmetry restoration. This discussion already indicates that a model dependence is introduced by the decomposition (6.1), (6.2). Clearly “bare nucleons” are not observable objects. We will come back to that point when we discuss our results in the last section.

Next we will perform a sum rule analysis for the correlators with respect to the system of bare nucleons  $R_{V/A}^b$  at nuclear saturation density  $\rho_N = 0.17/\text{fm}^3$ . Concerning the vector channel this is the essential difference as compared to our previous work [23] where we have analyzed the sum rule for the full in-medium correlator  $R_V$ . Note that Eqs. (2.14), (2.15) are valid for both full and bare correlators. The difference appears in Eq. (2.16) in the calculation of the expectation value with respect to bare or full nucleons, respectively. In practice, the difference manifests itself only in the different handling of the four-quark condensate. All OPE contributions in Eqs. (2.14) and (2.15) except from the two- and four-quark condensates come from chiral singlet operators. They do not distinguish between bare nucleons and nucleons dressed by soft pions. Hence their evaluation is standard [23]. Things are different for the two- and four-quark condensates. Concerning the two-quark condensate, its in-medium change (in linear density approximation) is determined by the nucleon sigma term (6.10). To calculate the in-medium change with respect to bare nucleons we have to take into account only  $\sigma_N^b$  as defined via Eq. (6.11):

$$\frac{\langle \bar{q}q \rangle_b}{\langle \bar{q}q \rangle_{\text{vac}}} = 1 - \frac{\sigma_N^b \rho_N}{f_\pi^2 m_\pi^2}. \quad (6.13)$$

In practice, the value of  $m_q \langle \bar{q}q \rangle$  is rather small (as compared to the gluon condensate) and further diminished in the medium. In contrast, the four-quark condensate is numerically important. In lack of a better access to the value of  $\mathcal{O}_4^V$  at finite density we made in Ref. [23] the common assumption that this four-quark condensate scales with the density as the square of the two-quark condensate

$$\langle \mathcal{O}_4 \rangle_{\text{med}} = \langle \mathcal{O}_4 \rangle_{\text{vac}} \left( \frac{\langle \bar{q}q \rangle_{\text{med}}}{\langle \bar{q}q \rangle_{\text{vac}}} \right)^2 = \langle \mathcal{O}_4 \rangle_{\text{vac}} \left( 1 - \frac{\sigma_N \rho_N}{f_\pi^2 m_\pi^2} \right)^2. \quad (6.14)$$

In the comparable case of finite temperature (i.e., in a hot pion gas), however, it was shown in Ref. [46] that such an assumption is wrong. This can be traced back to the fact that in the presence of pions the two-quark condensate behaves different as compared to the four-quark condensate due to its

different transformation properties with respect to chiral transformations. This suggests that also at finite nucleon density the scaling assumption (6.14) is doubtful due to the presence of virtual pions. In the present work we have explicitly taken into account the contribution from the pion cloud of the nucleons. In this way we have expressed the full correlator in terms of the bare correlators. We now assume the scaling property (6.14) only for the condensates with respect to a system of bare nucleons. It takes the form

$$\langle \mathcal{O}_4 \rangle_b = \langle \mathcal{O}_4 \rangle_{\text{vac}} \left( 1 - \frac{\sigma_N^b \rho_N}{f_\pi^2 m_\pi^2} \right)^2, \quad (6.15)$$

where for consistency we have to take the bare nucleon sigma term  $\sigma_N^b = \sigma_N - \sigma_N^\pi \approx 20$  MeV instead of the full one  $\sigma_N \approx 45$  MeV. In the following we use this scaling assumption (6.15) for both  $\langle \mathcal{O}_4^V \rangle_b$  and  $\langle \mathcal{O}_4^A \rangle_b$ .

In view of the uncertainty connected with the four-quark condensate it clearly would be fortunate to use sum rules which do not involve it. Indeed, in Ref. [43] the first two finite energy sum rules (3.1a), (3.1b) were used. However, with the same parameter set ( $m_\rho, \gamma, F, s_0$ ) characterizing the hadronic correlator the two sum rules are capable to determine only two of these four parameters. To further restrict the parameter space additional information is required. In Ref. [43] it is suggested that the threshold  $s_0$  is connected to the scale of chiral symmetry breaking. Thus, the choice is either to make assumptions about the four-quark condensate or about the threshold parameter. As outlined above we prefer to work with the Borel sum rule instead of the finite energy sum rules due to the larger sensitivity of the latter to the high-energy modeling. In this case we cannot get rid of the four-quark condensate.

The sum rule analysis proceeds along the same lines as described above for the vacuum case. We analyze the Borel sum rules for the  $\rho$  as well as the  $a_1$  meson placed in a medium of *bare* nucleons. For the timelike part of the correlator in the vector channel we use again a single resonance parametrization of type (4.1). For the axial-vector channel we recall that there is a pion branch in addition to the  $a_1$ . Here there is an additional change in the medium due to a change of the pion decay constant in nuclear matter. We replace  $f_\pi^2$  in Eq. (4.2) by

$$f_\pi^{*2} \approx f_\pi^2 \frac{\langle \bar{q}q \rangle_b}{\langle \bar{q}q \rangle_{\text{vac}}}, \quad (6.16)$$

where we have utilized the in-medium version of the Gell-Mann–Oakes–Renner relation (2.18) and neglected a possible in-medium change of the pion mass. By using Eq. (4.2) with the replacement (6.16) we also assume that the  $\delta$ -type spectral function of the pion is not significantly smeared out. In fact, pion properties are expected to change drastically in nuclear matter due to the strong coupling to  $\Delta$ -hole states [47]. However, this  $p$ -wave coupling is not important here since we deal with correlators which are at rest with respect to the nuclear environment. Working in the linear density approximation, i.e., neglecting Fermi motion, the pions do

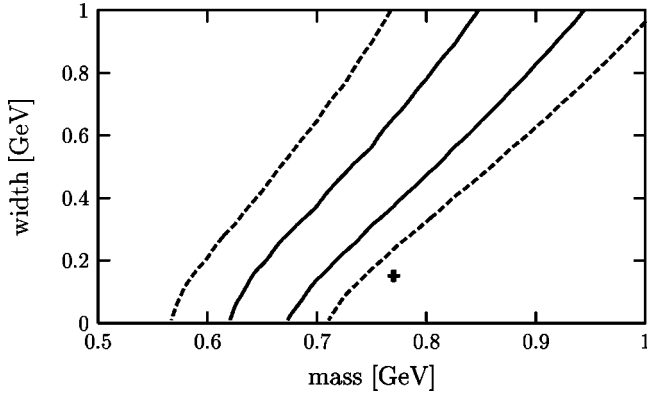


FIG. 6. Same as Fig. 2 for  $\rho$  in system of bare nucleons at normal nuclear matter density. For the calculation of the width the two-pion threshold is adopted. See text for details.

not couple to the nucleons by exciting  $\Delta$ 's. In the context of the (necessary) approximations involved it seems reasonable to work with a pion spectral function which is neither shifted nor broadened.

## VII. RESULTS FOR NUCLEAR MATTER

The results of the sum rule analysis are shown in Figs. 6, 7, and 8. As for the vacuum case we find bands of allowed mass-width pairs. The interesting point is how these bands have changed as compared to the respective vacuum case. As already mentioned concerning the choice for the vacuum four-quark condensate we have used the respective better value, i.e.,  $(-292 \text{ MeV})^6$  for the  $\rho$  meson and  $(-281 \text{ MeV})^6$  for the  $a_1$ . Hence we have to compare Figs. 6, 7 to Fig. 2 and Fig. 8 to Fig. 5.

For the  $\rho$  meson we have explored two possibilities to parametrize the energy dependence of the width. The same parametrization (4.5) as for the vacuum case, i.e., with the two-pion threshold, is used to obtain the results depicted in Fig. 6. Here the mass-width band is shifted to the left as compared to the vacuum case (Fig. 2). Obviously, the in-medium change of the condensates calls for more strength at lower invariant masses as compared to the situation in

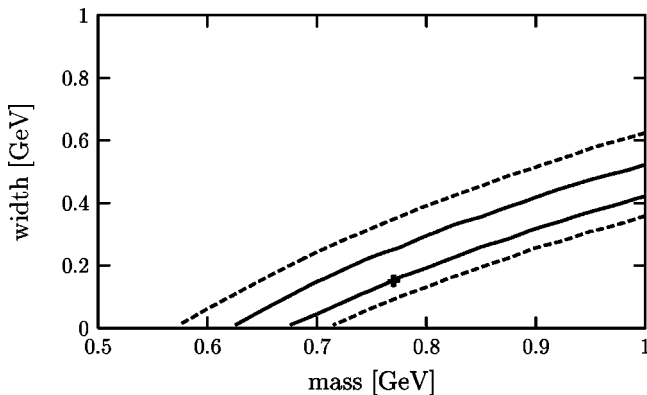


FIG. 7. Same as Fig. 2 for  $\rho$  in system of bare nucleons at normal nuclear matter density. For the calculation of the width the one-pion threshold is adopted. See text for details.

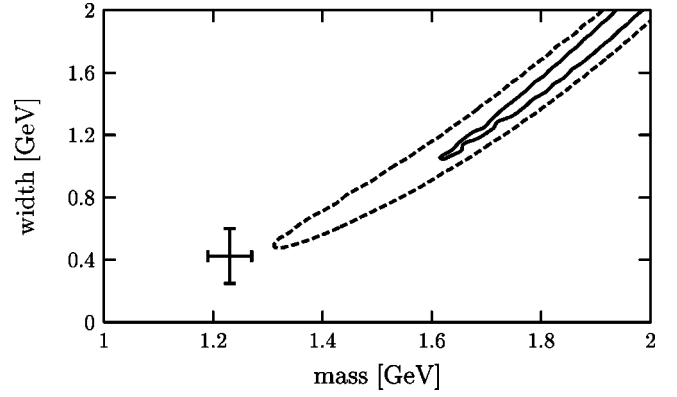


FIG. 8. Same as Fig. 5 for  $a_1$  in system of bare nucleons at normal nuclear matter density. For the calculation of the width the one-pion threshold is adopted. See text for details. Note the different scale for the width as compared to previous figures.

vacuum. This can be accomplished either by a lower peak mass or by a larger width. For Fig. 7 the parametrization (4.9) with the one-pion threshold is used. For very small width the masses allowed by the sum rule analysis agree for Figs. 6 and 7. This is of course due to the fact that the details of the off-shell parametrization of the width do not matter if the width is sufficiently small. For larger widths, however, there appear large differences between Figs. 6 and 7. The band in Fig. 7 is much less steep. This is easy to understand: The demand for more strength at lower invariant masses is easier to fulfill if there is already some strength below the two-pion threshold. Therefore, for the same peak mass the on-shell width can be smaller if the one-pion threshold is used instead of the two-pion threshold. The large differences between Figs. 6 and 7 stress again that the Borel sum rule is very sensitive to the low-energy behavior of the spectral distribution. More generally one has to realize that peak mass and on-shell width are sufficient to characterize a spectral function only if the width is not too large. For large width details of the spectral shape become important, in the case at hand especially the details in the low-energy region. Concerning the Borel mass window we get  $M_{\min}^2 = 0.64 \text{ GeV}^2$ . For all mass-width pairs in the inner bands of Figs. 6 and 7 and to the right of it we find  $M_{\max}^2 > 1.2 \text{ GeV}^2$ . It is a generic finding of sum rule analyses that the Borel window shrinks to some extent when changing from the vacuum to the in-medium case [23]. Still we regard the Borel window to be large enough to draw conclusions from the analysis.

Turning to the  $a_1$  meson Fig. 8 shows that the tendency of the sum rule to support large values of the width (see Fig. 5) increases in medium. (Note that the width scale in Fig. 8 differs from the previous figures.) The minimal Borel mass is given by  $M_{\min}^2 = 0.61 \text{ GeV}^2$  while  $M_{\max}^2 > 2.0 \text{ GeV}^2$  for the whole relevant mass-width range. For the width we have used parametrization (4.10) with the one-pion threshold to obtain Fig. 8. We have also analyzed the sum rule using instead Eq. (4.7) with the rho-pion threshold. In this case we did not find any mass-width pair with a deviation  $d$  less than 1%. Therefore, we do not show a plot for the latter case. In fact, even if we allowed for larger values of  $d$  there would be no sign for the desired mass-width band. We conclude that

parametrization (4.7) is incompatible with the in-medium sum rule for the  $a_1$  meson. Obviously this sum rule demands for a spectral distribution which is smeared out over a large invariant mass range. Restricting the mass range by a (rather high) lower limit of  $m_\pi + m_\rho \approx 0.9$  GeV appears to be insufficient to fulfill the sum rule. Instead, the one-pion threshold (caused by nucleon- $a_1$  collisions) does the job. Of course, also other scenarios which might fulfill the sum rule are conceivable. As we have learned from the previous in-medium sum rule analysis the spectral function of the  $\rho$  meson gains strength at lower invariant mass (either by a lower peak mass or by a larger width). Thus the effective threshold for the in-medium decay of the  $a_1$  meson into rho plus pion is probably lowered as compared to the vacuum case. Such a scenario might also be in line with the sum rule. We have not explored this possibility in further detail since we would have to introduce a couple of new free parameters to model, e.g., the successive in-medium decays  $a_1 \rightarrow \rho + \pi \rightarrow 3\pi$ . As already noticed when discussing the results for the  $\rho$  meson we find also for the  $a_1$  that the QCD sum rule is sensitive to the threshold modeling of the width provided that the on-shell width is not too small. This fact has not been sufficiently taken into account in Ref. [48] leading to results for the  $a_1$  meson which differ from the ones presented here. We also deduce from Fig. 8 that the nominal peak mass is shifted to higher values. It is important to note that this shift is *not* in contradiction to chiral symmetry. What we have studied so far is the behavior of the correlators under the influence of the system of *bare* nucleons. Chiral symmetry only demands that the *full* correlators of the vector and axial-vector channel become degenerate at high enough density. This is achieved by the pions as expressed by the mixing formula (6.12) no matter how the  $a_1$  mass changes under the influence of the bare nucleons.

To visualize the effect of mixing we now turn to the full in-medium correlators obtained from the bare ones via Eq. (6.7). As already pointed out the sum rule analysis in general is not capable to pin down both in-medium mass and width for the respective meson. Nonetheless, to illustrate the effect of mixing we arbitrarily take one pair of values for the  $\rho$  meson from the inner band depicted in Fig. 7 and the optimal pair for the  $a_1$  meson. We choose

$$m_\rho = 0.77 \text{ GeV}, \quad \gamma_\rho = 0.21 \text{ GeV}, \quad s_0^\rho = 1.15 \text{ GeV}^2, \\
 F_\rho = 1.1 \times 10^{-2} \text{ GeV}^4; \quad (7.1a)$$

$$m_{a_1} = 1.86 \text{ GeV}, \quad \gamma_{a_1} = 1.67 \text{ GeV}, \\
 s_0^{a_1} = 3.84 \text{ GeV}^2, \quad F_{a_1} = 0.36 \text{ GeV}^4. \quad (7.1b)$$

The results for the imaginary part of the full in-medium vector and axial-vector correlators are shown in Figs. 9 and 10 together with the respective contributions from the bare correlators. In the figures we have not included the delta function type contributions from the pion and from Landau damping. Note that the shoulder of the  $\rho$  contribution at low invariant mass is caused by the  $1/s$  factor present in Eq. (4.1). Especially the axial-vector correlator shows that in the

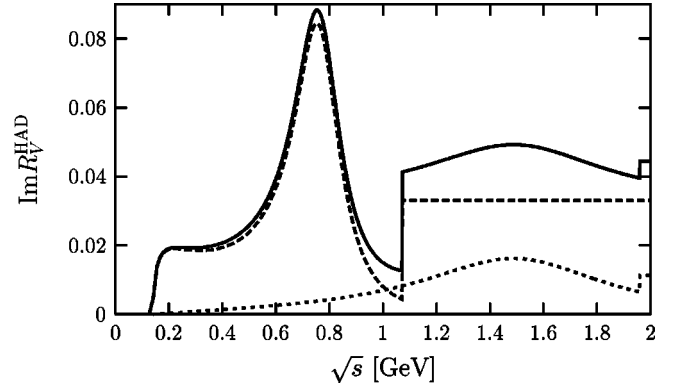


FIG. 9. Imaginary part of the full in-medium vector correlator (full line) as a function of  $\sqrt{s} = \sqrt{q^2}$ . The contribution of the bare vector (axial-vector) correlator is given by the dashed (dotted) line. See text for details.

medium the resonance peaks are no longer higher than the high energy continuum. Recalling that the modeling of the onset of the continuum is rather crude one might further soften the crossover regions leaving basically no room for distinct peak structures. In total, we see a clear sign that the in-medium spectral distributions get washed out with increasing density.

## VIII. SUMMARY

We have presented a QCD sum rule analysis for the in-medium current-current correlators with the quantum numbers of  $\rho$  and  $a_1$  mesons. For the medium we have chosen the case of a Fermi gas of nucleons at vanishing temperature. For comparison we have also presented the vacuum sum rule analysis for  $\rho$  and  $a_1$ . As possible in-medium changes for the spectral distributions of both correlators we have allowed for mass shifts, peak broadening, and also mixing. The latter effect has not been considered in previous analyses [18,19,23].

In the QCD sum rule only a mass-averaged quantity involving the respective spectral distribution enters. In general the sum rule is not capable to pin down the full information

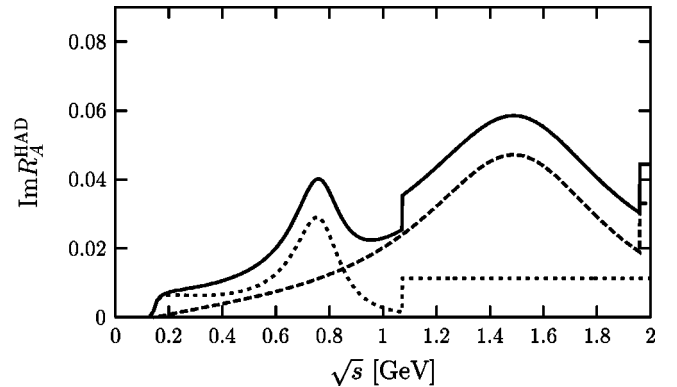


FIG. 10. Imaginary part of the full in-medium axial-vector correlator (full line) as a function of  $\sqrt{s} = \sqrt{q^2}$ . The contribution of the bare axial-vector (vector) correlator is given by the dashed (dotted) line. See text for details.

present in the spectral distribution such as the number of peaks, their positions, widths, and heights. Therefore one needs an ansatz for the spectral distribution with some free parameters. These parameters can be constrained by the requirement that the spectral distribution has to fulfill the sum rule. The simplest ansatz consists of only one peak (in the low-energy regime) and neglecting its width. In this case the sum rule for the  $\rho$  meson demands an in-medium mass shift towards smaller masses [18,19]. At normal nuclear matter density the mass has to drop by roughly 16%. This, however, is a model-dependent statement since a specific choice for the form of the spectral distribution has been made, namely, only one peak with vanishing width. In fact, if also the width is included but still using a one-peak ansatz it is already impossible to fix both the mass and the width. One obtains a band of allowed mass-width pairs [23]. At small width this band of course has to start at the mass determined in Refs. [18,19]—provided the same condensate values are used (see Ref. [23] for details). For larger widths the allowed masses also increase. With increasing nucleon density the mass-width band is shifted to the left, i.e., for a given value of the width to smaller masses.

If the true in-medium spectral distribution possesses more than one peak but in the ansatz for that quantity only one peak was present then certain in-medium changes caused by the additional peaks would be erroneously attributed to changes of mass and/or width of the single peak. Therefore, in the present work we have made a further step to consider all possible in-medium modifications. The mixing of the vector with the axial-vector correlator by the virtual nuclear pions has been included. Using soft pion techniques this mixing can be approximately calculated for the correlators irrespective of the choice for the correlator momentum  $q$ . Therefore the correlators can be decomposed into a superposition of “bare” correlators for both the OPE side ( $q^2 \ll 0$ ) and the spectral distribution ( $q^2 > 0$ ). In this way we have split off the mixing phenomena (at least the one induced by nuclear pions) from the sum rule analysis. Successively the latter has been applied to the bare correlators. As compared to previous works we have obtained a less drastic in-medium shift of the allowed mass-width band for the  $\rho$  branch. For the  $a_1$  branch we have found that the sum rule is better fulfilled for not too small values of the width. The preference of large widths increases with increasing density. We have also seen that for both the  $\rho$  and  $a_1$  meson at larger widths the respective sum rule is sensitive to the threshold modeling of the energy dependence of the width. Therefore, it appears to be insufficient to characterize a peak in the spectral distribution by its position and on-shell width. A reasonable modeling of the energy dependence of the width is important to obtain meaningful results from a QCD sum rule analysis.

As already mentioned we have found that there is a smaller in-medium shift of the mass-width band for the  $\rho$  meson as compared to the old analysis which did not include the mixing phenomena. At first glance this is a striking result. Suppose that the old analysis is polluted by an additional  $a_1$  peak, i.e., a peak at large invariant masses. First of all, one might argue that this additional peak is suppressed by the exponential function appearing in Eq. (2.9). Therefore

this peak should not drastically modify the analysis for the  $\rho$  meson as generally assumed for all details of the high-energy part. Note that Figs. 9 and 10 show that in general the position of the  $a_1$  peak is beyond the onset of the continuum of the  $\rho$  branch, see also Eq. (7.1). Let us ignore that point for a moment and face a second apparent contradiction of our results to naive expectations. Consider the influence of the additional  $a_1$  peak on the determined mass (for a given width). Clearly the mass which we have attributed to the  $\rho$  meson in the old analysis would be a weighted average of the true  $\rho$  peak and the  $a_1$  peak. Therefore the true  $\rho$  peak should be at smaller mass values as compared to the result of the old analysis. In the present analysis, however, we have found just the opposite result. The solution to these apparent contradictions is the appearance of the pion in the axial-vector branch. It is not the high lying  $a_1$  but the low lying pion which has dominantly pollutes the old analysis. Since the pion is much lighter than the  $\rho$  the former has caused a too large shift of the mass-width band to the left in the old analysis. The  $a_1$  peak plays only a subdominant role as expected from modifications in the high-energy regime.

After the decomposition of the full correlators into bare ones we have tacitly assumed that for the latter the one-peak ansatz for (the low-energy part of) the spectral distribution is reasonable. In fact, also this assumption appears to be questionable due to the coupling of the  $\rho$ -nucleon system to resonances (see, e.g., Refs. [38,39], and references therein). Especially the apparently sizable coupling to the  $D_{13}$  resonance  $N^*(1520)$  might create an additional peak at an invariant mass of roughly 580 MeV, i.e., below the vacuum  $\rho$  peak<sup>9</sup>—provided that the resonance mass does not change in the nuclear medium. Therefore, e.g., our result for the in-medium mass-width band of the  $\rho$  branch might still be polluted by the influence of additional distinct peaks. We have refrained from including more than one peak in the ansatz for the spectral distribution since we would have been forced to introduce much more free parameters which cannot be determined from the sum rule. Further work is necessary to separate the different peaks. On the other hand, we have already seen that the present sum rule analysis supports broad in-medium spectral functions. It may appear that the baryonic resonances also melt in a nuclear environment (see, e.g., Ref. [49], and references therein) and leave no sign of distinct peaks in the mesonic channels.

Concerning the included mixing effect of the vector and axial-vector channel the amount of mixing is determined by the value for  $\sigma_N^\pi$ . As we have already mentioned even the sign of that quantity is still subject to discussion. Therefore it is important to stress that the presented calculations are by no means free of model assumptions. The reason is that the separation of nuclear matter into bare nucleons and soft

<sup>9</sup>Note that only resonances with an  $s$ -wave coupling to  $N$ - $\rho$  can contribute for the case at hand since we have considered  $\rho$  mesons at rest with respect to the nuclear medium. On account of the linear density approximation we have neglected the Fermi motion of the nucleons.

pions is a model dependent concept as an extrapolation in the off-shell region, i.e., to virtual pions is involved here. Unless one can estimate  $\sigma_N^\pi$  in a model independent way with unambiguous sign the mixing effect at finite density remains to be a controversial issue. This is actually in contrast to the case of finite temperature where the heat bath is modeled by a gas of real pions. Hence the so far unavoidable model dependence which enters the calculation for finite nuclear density is absent at finite temperature. In the calculations the influence of  $\sigma_N^\pi$  is twofold. First, it yields the amount of mixing on account of Eq. (6.7). Here a change of  $\sigma_N^\pi$  does not influence the sum rule analysis for the bare correlators but it does influence the final result for the full correlators exemplified in Figs. 9 and 10. Especially if  $\sigma_N^\pi$  was negative one could no longer guarantee that the sign of the imaginary parts of the full correlators remains positive for all values of the invariant mass  $\sqrt{s}$ . In this case the approximations which have led to Eq. (6.7) should be revised.

The second place where  $\sigma_N^\pi$  appears is the in-medium dependence of the quark condensates. Most importantly, it enters the scaling assumption (6.15) for the four-quark condensate via Eq. (6.11). We have made this assumption in lack of any better, more fundamental approach. One might corroborate our choice by the expectation that factorization roughly works as long as there is no fundamental (symmetry) principle which is in contradiction to factorization. In our case the interaction with the pions is determined by chiral symmetry. Here factorization breaks down as proven for the case of finite temperature in Ref. [46]. Having split off the pions one might expect that the factorization assumption works for the interaction of the vector and axial-vector mesons with the bare nucleons. Nonetheless it is important to figure out how important the influence of the four-quark condensate and especially of its in-medium change actually is: At a typical value for the Borel mass of  $M \approx 1$  GeV we find

the following in-medium changes on the OPE side of the  $\rho$  meson sum rule at nuclear saturation density: The important changes are induced by the twist-two condensate with dimension 4,  $2.7 \times 10^{-4}$ , and the in-medium change of the four-quark condensate,  $1.5 \times 10^{-4}$ . All other changes are an order of magnitude smaller:  $-3.6 \times 10^{-5}$  from the in-medium change of the gluon condensate,  $1.3 \times 10^{-5}$  from the in-medium change of the two-quark condensate,  $-2.7 \times 10^{-5}$  from the twist-two condensate with dimension 6. Therefore even if the change of the four-quark condensate was completely neglected roughly two thirds of the in-medium change would still persist. Thus, the results obtained here would not drastically change. The vacuum contribution of the four-quark condensate is  $-4.8 \times 10^{-4}$ . If the four-quark condensate vanished completely at nuclear saturation density the in-medium change would be twice as large as the one used in our analysis. One should realize that the previous considerations are somewhat oversimplified as the dependence on the Borel mass is different for the OPE contributions from the dimension-4 condensates as compared to the ones with dimension 6. In total, however, we do not expect qualitative changes of the picture presented here even if the in-medium behavior of the four-quark condensate was completely different.

In spite of the large uncertainties connected with the QCD sum rule method at finite baryon density we regard it as a useful complement to purely hadronic approaches since it connects in a unique way hadronic with quark-gluon degrees of freedom. We hope that the mentioned uncertainties can be removed step by step in the future.

#### ACKNOWLEDGMENTS

The author wants to thank Ulrich Mosel for discussions and continuous support. This work was supported by GSI Darmstadt and BMBF.

- 
- [1] L. Riccati, M. Masera, and E. Vercellin, *Proceedings of the 14th International Conference on Ultra-relativistic Nucleus-Nucleus Collisions, QM'99*, Torino, Italy [Nucl. Phys. **A661**, 1 (1999)].
  - [2] M. A. Shifman, A. I. Vainshtein, and V. I. Zakharov, Nucl. Phys. **B147**, 385 (1979); **B147**, 448 (1979).
  - [3] L. J. Reinders, H. Rubinstein, and S. Yazaki, Phys. Rep. **127**, 1 (1985).
  - [4] M. Dey, V. L. Eletsky, and B. L. Ioffe, Phys. Lett. B **252**, 620 (1990).
  - [5] J. I. Kapusta and E. V. Shuryak, Phys. Rev. D **49**, 4694 (1994).
  - [6] R. Pisarski, Phys. Rev. D **52**, R3773 (1995).
  - [7] G. Agakichiev *et al.*, CERES Collaboration, Phys. Rev. Lett. **75**, 1272 (1995); A. Drees for the CERES Collaboration, Nucl. Phys. **A630**, 449c (1998); G. Agakichiev *et al.*, CERES Collaboration, Phys. Lett. B **422**, 405 (1998).
  - [8] N. Masera for the HELIOS-3 Collaboration, Nucl. Phys. **A590**, 93c (1995).
  - [9] V. Koch and C. Song, Phys. Rev. C **54**, 1903 (1996).
  - [10] G. E. Brown and M. Rho, Phys. Rev. Lett. **66**, 2720 (1991).
  - [11] G. Q. Li, C. M. Ko, and G. E. Brown, Phys. Rev. Lett. **75**, 4007 (1995); Nucl. Phys. **A606**, 568 (1996).
  - [12] W. Cassing and E. L. Bratkovskaya, Phys. Rep. **308**, 65 (1999).
  - [13] R. Rapp and J. Wambach, hep-ph/9909229.
  - [14] K. G. Wilson, Phys. Rev. **179**, 1499 (1969).
  - [15] T. Hatsuda, Y. Koike, and S. H. Lee, Nucl. Phys. **B394**, 221 (1993).
  - [16] V. L. Eletsky and B. L. Ioffe, Phys. Rev. D **51**, 2371 (1995).
  - [17] V. L. Eletsky, P. J. Ellis, and J. I. Kapusta, Phys. Rev. D **47**, 4084 (1993).
  - [18] T. Hatsuda and S. H. Lee, Phys. Rev. C **46**, R34 (1992).
  - [19] T. Hatsuda, S. H. Lee, and H. Shiomi, Phys. Rev. C **52**, 3364 (1995).
  - [20] F. Klingl, N. Kaiser, and W. Weise, Nucl. Phys. **A624**, 527 (1997).
  - [21] M. Asakawa, C. M. Ko, P. Lévai, and X. J. Qiu, Phys. Rev. C **46**, R1159 (1992).
  - [22] M. Asakawa and C. M. Ko, Phys. Rev. C **48**, R526 (1993).

- [23] S. Leupold, W. Peters, and U. Mosel, Nucl. Phys. **A628**, 311 (1998).
- [24] S. Leupold and U. Mosel, Phys. Rev. C **58**, 2939 (1998).
- [25] T. Schäfer and E. V. Shuryak, Rev. Mod. Phys. **70**, 323 (1998).
- [26] V. L. Eletsky and B. L. Ioffe, Phys. Rev. Lett. **78**, 1010 (1997).
- [27] T. Hatsuda and S. H. Lee, nucl-th/9703022.
- [28] V. L. Eletsky and B. L. Ioffe, hep-ph/9704236.
- [29] B. Friman, S. H. Lee, and H. Kim, Nucl. Phys. **A653**, 91 (1999).
- [30] D. B. Leinweber, Ann. Phys. (N.Y.) **254**, 328 (1997).
- [31] X. Jin and D. B. Leinweber, Phys. Rev. C **52**, 3344 (1995).
- [32] P. Pascual and R. Tarrach, *QCD: Renormalization for the Practitioner*, Vol. 194 of Lecture Notes in Physics (Springer, Berlin, 1984).
- [33] G. Chanfray and P. Schuck, Nucl. Phys. **A545**, 271c (1992); **A555**, 32 (1993).
- [34] M. Herrmann, B. Friman, and W. Nörenberg, Nucl. Phys. **A545**, 267c (1992); **A560**, 411 (1993).
- [35] R. Rapp, G. Chanfray, and J. Wambach, Phys. Rev. Lett. **76**, 368 (1996).
- [36] B. Friman and H. J. Pirner, Nucl. Phys. **A617**, 496 (1997).
- [37] R. Rapp, G. Chanfray, and J. Wambach, Nucl. Phys. **A617**, 472 (1997).
- [38] W. Peters, M. Post, H. Lenske, S. Leupold, and U. Mosel, Nucl. Phys. **A632**, 109 (1998).
- [39] M. Post, S. Leupold, and U. Mosel, nucl-th/0008027.
- [40] W. Florkowski and W. Broniowski, Nucl. Phys. **A651**, 397 (1999).
- [41] S. H. Lee, Phys. Rev. C **57**, 927 (1998).
- [42] K. Maltman, Phys. Lett. B **440**, 367 (1998).
- [43] E. Marco and W. Weise, Phys. Lett. B **482**, 87 (2000).
- [44] B. Krippa, Nucl. Phys. **A672**, 270 (2000).
- [45] G. Chanfray, J. Delorme, M. Ericson, and M. Rosa-Clot, nucl-th/9809007.
- [46] V. L. Eletsky, Phys. Lett. B **299**, 111 (1993).
- [47] T. Ericson and W. Weise, *Pions and Nuclei* (Clarendon, Oxford, 1988).
- [48] S. Leupold, in *Hadrons in Dense Matter, Hirscheegg 2000 Proceedings*, edited by M. Buballa, W. Nörenberg, B.-J. Schäfer, and J. Wambach (GSI, Darmstadt, 2000).
- [49] U. Mosel, Prog. Part. Nucl. Phys. **42**, 163 (1999).
- [50] Particle Data Group, C. Caso *et al.*, Eur. Phys. J. C **3**, 1 (1998).